

How the Liquid-Liquid Transition Affects Hydrophobic Hydration in Deeply Supercooled Water

Dietmar Paschek*

Physikalische Chemie, Universität Dortmund, Otto-Hahn-Str. 6, D-44221 Dortmund, Germany

(Dated: May 23, 2019)

We determine the phase diagram of liquid supercooled water by computer simulation. Extensive Volume-Temperature Replica Exchange Molecular Dynamics (VTREMD) simulations over a broad temperature (170 K to 356 K) and density (0.890 g cm^{-3} to 1.205 g cm^{-3}) range using of a grid of 440 states are reported. This parallel tempering approach allows a proper thermodynamical sampling of the states even for the highly viscous liquid down to 170 K. The employed TIP5P-E model (J. Chem. Phys. **120**, 6085 (2004)) reveals the presence of a second critical point located at a positive pressure of 310 MPa at 210 K and 1.09 g cm^{-3} . We find that the transformation of water into a low density liquid strongly enhances the solubility of hydrophobic particles. In addition, the apparent transformation of water into a tetrahedrally structured liquid at lower temperatures is accompanied with a minimum in the hydrophobic hydration entropy. The corresponding change in sign of the solvation heat capacity indicates a loss of one characteristic signature of hydrophobic hydration. The observed behavior is found to be qualitatively in accordance with the predictions of the information theory model of Garde et al. (Phys. Rev. Lett. **77**, 4966 (1996)).

The thermodynamical anomalies of liquid water are considered to be caused by a transformation between two different liquid forms of water buried in the deeply supercooled region [1]. The two differently dense liquids have well characterized counterparts in the glassy state: The (very) high density and low density amorphous ice forms [2, 3]. Computer simulation studies have furnished a picture of a first order liquid-liquid phase transition between two liquids ending up in a metastable critical point [4, 5]. Although singularity free scenarios might as well explain the properties of supercooled water [1], there is experimental support for the liquid-liquid critical point hypothesis from the changing slope of the metastable melting curves observed for different ice polymorphs [6, 7]. To make the situation even more puzzling, recent computer simulations provide evidence that there might be even more than one liquid-liquid transition [8].

One prominent anomaly of liquid water is the increasing solubility of hydrophobic gases with decreasing temperature [9]. This behavior is the consequence of a negative solvation entropy of small hydrophobic particles [10]. Since the corresponding solvation enthalpy is also negative, the observed low solubility (the large positive solvation free energy) of small hydrophobic particles is basically due to a strong entropy effect. The origin of the negative hydration entropy is widely regarded as being due to the bias in the hydration waters orientational space, as the water molecules are trying to preserve their hydrogen bond network [11]. Entropy and enthalpy effects have been shown to be determined by the water in the first hydration shell [12]. In addition, the broken hydrogen bond states, with hydrogen bond donors/acceptors pointing towards the hydrophobic particles, are increasingly populated with increasing temperature [11]. Hence hydrophobic particles exhibit a *positive* solvation heat capacity, which is seen as one of the key signatures for hy-

drophobic hydration [13]. A recent experimental study of Souda [14] investigating alkane layers adsorbed on an amorphous solid water substrate, shows that the alkane phase gets soaked into the water phase in the temperature region close to the suspected glass transition temperature [15]. One possible explanation (among others) might be that the highly viscous low density liquid form of water provides a significantly increased solubility for hydrophobic molecules. The scope of the present contribution is to monitor hydration of a small hydrophobic particle as we penetrate the deeply supercooled region. Our particular interest is to elucidate how the transformation into a low density, highly tetrahedrally ordered liquid phase [16] affects hydrophobic hydration.

The technical key problem regarding simulations of highly viscous liquids close to the glass transition is, of course, to provide proper sampling. To overcome this problem we perform parallel tempering simulations of an extended ensemble of states [17]. Here we use the technique of volume-temperature replica exchange molecular dynamics simulation (VTREMD), which has been recently introduced by us to study the reversible pressure/temperature induced unfolding of small proteins [18]. To represent liquid supercooled water we employ the recently proposed TIP5P-E model for water, which was fitted to reproduce waters density maximum and related thermodynamical anomalies as closely as possible while treating the Coulomb interactions with the Ewald sum [19]. For the VTREMD simulation [20] we consider a grid of 440 (V, T)-states, each state characterized by its volume V and temperature T . The considered state-points are represented by the temperatures 170.0 K, 181.6 K, 192.8 K, 203.5 K, 213.5 K, 222.7 K, 230.8 K, 238.0 K, 244.8 K, 251.8 K, 259.1 K, 266.9 K, 275.2 K, 284.2 K, 293.8 K, 304.3 K, 315.5 K, 327.8 K, 341.3 K and 356.3 K at the densities 0.890 g cm^{-3} , 0.905 g cm^{-3} , 0.920 g cm^{-3} ,

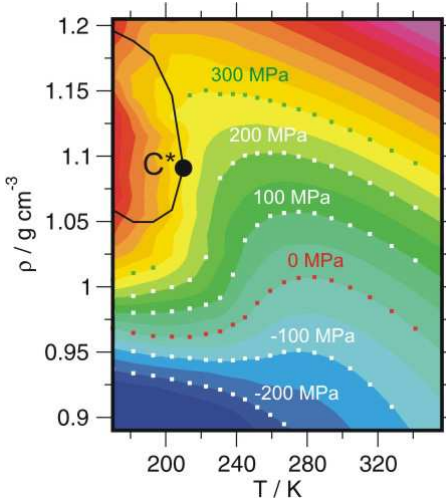


FIG. 1: Phase diagram for stable and supercooled liquid TIP5P-E water according to the VTREMD $P(\rho, T)$ data set. The spacing between different contour colours is according to a pressure drop of 50 MPa. Selected isobars are indicated. The high density liquid / low density liquid (LDL/HDL) coexistence line is given by the black solid line. The corresponding HDL/LDL critical point is denoted by C^* with $T^* = 210$ K, $P^* = 310$ MPa and $\rho^* = 1.09$ g cm $^{-3}$.

0.935 g cm $^{-3}$, 0.950 g cm $^{-3}$, 0.965 g cm $^{-3}$, 0.980 g cm $^{-3}$, 0.995 g cm $^{-3}$, 1.010 g cm $^{-3}$, 1.025 g cm $^{-3}$, 1.040 g cm $^{-3}$, 1.055 g cm $^{-3}$, 1.070 g cm $^{-3}$, 1.085 g cm $^{-3}$, 1.100 g cm $^{-3}$, 1.115 g cm $^{-3}$, 1.130 g cm $^{-3}$, 1.145 g cm $^{-3}$, 1.160 g cm $^{-3}$, 1.175 g cm $^{-3}$, 1.190 g cm $^{-3}$ and 1.205 g cm $^{-3}$. Starting from set a of equilibrated initial configurations obtained at ambient conditions, the VTREMD simulation [21] was conducted for 20 ns, providing a total 8.8 μ s worth of trajectory data. The average time interval between two successful exchanges was obtained to be about 3 ps. During the entire course of the simulation each replica has crossed the whole temperature and density interval several times. Quickly, after an initial equilibration period of about 4 ns, the average pressure and potential energies show convergence even for the lowest temperatures and the remaining 16 ns is used for analysis.

Figure 1 shows the phase diagram of liquid supercooled water in terms of a contour plot of the $P(\rho, T)$ -data as obtained by the VTREMD simulations. The TIP5P-E phase diagram exhibits a first order phase transition between two metastable liquid phases, ending in a second critical point C^* . The location of C^* as obtained here for the TIP5P-E model is very close the values reported by Yamada et al. for the original TIP5P model with $T^* = 217$ K, $P^* = 340$ MPa and $\rho^* = 1.13$ g cm $^{-3}$ [23]. Figure 2a compares several selected isobars as obtained by linear interpolation from the TIP5P-E $P(\rho, T)$ data set with the experimental data according to Wagner and Prüß [22]. Although the location of the density maximum at normal pressure is close to the experimental values,

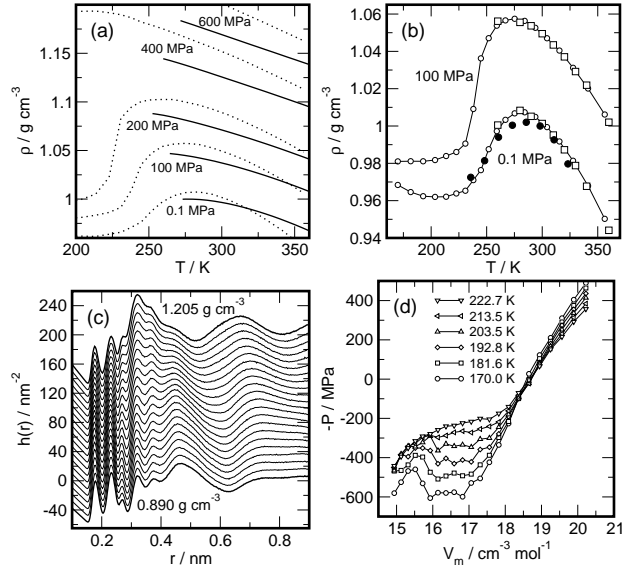


FIG. 2: (a): Selected isobars for TIP5P-E water (dotted lines) compared with experimental data of Ref. [22]. (b) Two isobars for TIP5P-E. Open circles: Data obtained by linear interpolation from the VTREMD $P(V, T)$ data set. Open squares: Data obtained by conventional constant temperature/constant pressure MD simulations. Filled circles: Data according to S. W. Rick [19]. (c) $h(r) = 4\pi r(N/V) [0.092 g_{OO}(r) + 0.486 g_{HH}(r) + 0.422 g_{OH}(r) - 1]$ -functions for the 222.7 K isotherm. The functions are shifted by an increment of 10 nm $^{-2}$. (d) Van-der-Waals loops of the sub-critical isotherms.

the TIP5P-E model indicates a considerably larger thermal expansivity as the real water and is significantly less compressible. Figure 2b shows that the isobars obtained the VTREMD data set match exactly with data obtained from conventional NPT -simulations. In addition the isobar according to S. W. Rick is shown [19]. We denote small, but significant differences. Since both data sets were obtained from simulations employing Ewald summation, we can just speculate about their origin. One explanation might be a possible absence of long range Lennard-Jones pressure corrections in Ref. [19]. We would like to emphasize one particular detail of the lower pressure isobars as indicated in Figures 1 and 2b: The density-isobars go through a minimum after the transformation into the low density liquid has taken place. Apparently the low density liquid expansivity seems to behave as it would be expected for a conventional liquid. I. Brovchenko [8] and recently P. H. Poole [24] have recently made a similar observations for the ST2-model. Figure 2c shows the evolution of the composite radial distribution function $h(r)$ along the 222.7 K-isotherm. The highlighted patterns obtained for the lowest and highest densities show strong similarity with the functions determined experimentally by Bellissent-Funel et al. for high density and low density amorphous ice [25]. The observed low density pattern has been shown to be con-

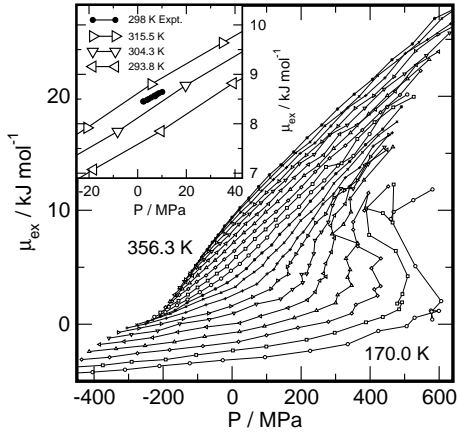


FIG. 3: Excess chemical potential for Ar dissolved in TIP5P-E water as a function of pressure and temperature. The lines indicate all calculated isotherms ranging from 170 K to 356.3 K. The insert shows the experimental data for 298 K according to Ref. [27] and the simulated isotherms lying close by.

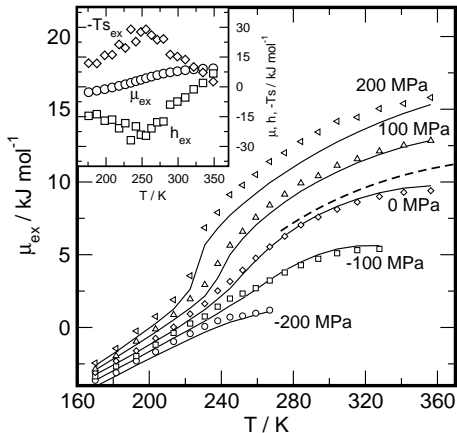


FIG. 4: The symbols indicate five representative isobars obtained by linear interpolation from the $\mu_{ex}(\rho, T)$ TIP5P-E data set. The dashed line indicates experimental data obtained for 0.1 MPa [28]. The full lines indicate μ_{ex} according to the leading term in the information theory model [29]. The insert shows the enthalpy (h_{ex}) and entropy ($-T s_{ex}$) contributions to the excess chemical potential for the simulated 0 MPa isobar.

nected with a highly tetrahedral order in the first hydration shell around each water molecule [16]. Similarities between the local structure of LDA and ice *Ih* have also been demonstrated recently by Finney et al. from the analysis of neutron scattering experiments [26]. Finally we would like to point out that we do not observe indications for the presence of further liquid-liquid transitions for TIP5P-E, as suggested by Brovchenko et al. for the ST2 model [8]. However, further phase transitions might be present at even lower temperatures.

The hydrophobic hydration of a Lennard-Jones Ar-gon particle ($\sigma_{\text{Ar-O}} = 0.3290 \text{ nm}$ and $\epsilon_{\text{Ar-O}}/k = 98.9 \text{ K}$) [30] is obtained in terms of the excess chemical potential

$\mu_{ex} = -\beta^{-1} \ln \gamma$ for infinite dilution, where γ is the solubility and $\beta = 1/kT$. We employ the Widom particle insertion method [17] with $\mu_{ex} = -\beta^{-1} \langle \exp(-\beta \Phi) \rangle$, where Φ is the energy of an inserted test-particle. The brackets $\langle \dots \rangle$ indicate canonical sampling. Details about the calculation are given elsewhere [30]. Figure 3 shows the excess chemical potential for Argon dissolved in TIP5P-E water obtained for all simulated state points as a function of temperature and pressure. First of all we would like to emphasize the fact the the solubility of the hydrophobic particle increases strongly when penetrating the deeply supercooled region with μ_{ex} becoming even *negative*. The insert of Figure 3 compares the available experimental data of Kennan and Pollack [27] with the simulation data. Although the experimentally available pressure interval is much smaller compared to the pressure range considered in our study, the almost quantitative coincidence is quite remarkable. The most prominent feature, the decreasing solubility with increasing pressure is found to be well reproduced. The pressure dependence, revealing a positive partial molar volume of $30 \text{ cm}^3 \text{ mol}^{-1}$ is quite close to the experimental value of $25 \text{ cm}^3 \text{ mol}^{-1}$ [31]. Two regimes of small and strong pressure dependence are denoted, obviously related to the transformation between the high and low density liquid forms of water. We would like to emphasize that we find an increase of the partial molar volume for Ar around normal pressure for the $260-255 \text{ K}$ isotherms. We would like to point out that Kennan and Pollack made a similar observation for Xenon around 298 K. If, and how these two observations are related has to be further investigated. Figure 4 shows the temperature dependence of μ_{ex} for several selected isobars ranging from -200 MPa to 200 MPa . The 0.1 MPa isobar according to Fernandez-Prini and Crovetto [28] is given for comparison. From computer simulations of water, S. Garde et al. have derived an information theory (IT) model [29, 32], giving simple analytic expressions for the hydrophobic hydration as a function of temperature and density. For the high temperature regime their approach has been shown to work almost quantitatively [29]. The leading term in the IT model strongly suggests a quadratic relation between the excess chemical potential and the water number density according to $\mu_{ex}/k \approx \rho^2 T v^2 / 2\sigma_n^2$ [32], where v denotes the volume of the size of a hydrophobic hard sphere particle, while $\sigma_n^2 = \langle n^2 \rangle - \langle n \rangle^2$ indicates the variance of the number of water molecules in a sphere of volume v . The lines in Figure 4 indicate a temperature dependence as suggested by the information theory model, assuming the term $v^2/2\sigma_n^2$ as being constant (and the same for all isobars shown here) and shifting the isobars by a constant offset to account for attractive interactions. The relation apparently describes the temperatures also for the supercooled state in an almost quantitative fashion over a very broad pressure range. Particularly well reproduced is the change in slope when passing the trans-

formation into the low density liquid. In addition, as shown in the insert of Figure 4 for the 0 MPa isobar, the change in slope is related the temperature dependence of the entropy and enthalpy contributions. The transformation is apparently related with a minimum in the hydration entropy and enthalpy. Furthermore, the minimum in the enthalpy causes a change in sign of the corresponding heat capacity contribution from positive at high temperatures to negative for the low density liquid. Apparently, a prominent signature of the “hydrophobic hydration” vanishes while passing the transition at about 250 K. In line with the interpretation of hydrophobic effects as derived from of the simplified MB model for water [11] at ambient conditions, the scenario might be explained as follows: In the low-temperature/low-density regime, waters coordination number approaches four, while the structure is that of a very homogeneous tetrahedral network. Hence, due to the lack of further possible hydrogen binding binding partners, the situation for a water molecules in the bulk or in the hydrophobic hydration shell might be less different than it is in the “high density liquid” at high temperatures. Consequently, a larger hydrophobic particle might even introduce further disorder into the stretched hydrogen hydrogen bond network and might thus even experience a *positive* hydration entropy. Therefore, a further investigation on particle size dependence, hydrophobic aggregates and hydrophobic interaction might reveal a behavior different from that supposed for ambient conditions [33] and thus could provide even more new insights in the phenomena of the hydrophobic effects.

This work was supported by DFG FOR 436. I would like to thank Angel E. García, Ivan Brovchenko and Alfonso Geiger for valuable discussions.

* Electronic address: dietmar.paschek@udo.edu

- [1] P. G. Debenedetti, *J. Phys. Cond. Matt.* **15**, R1669 (2003).
- [2] O. Mishima, L. D. Calvert, and E. Whalley, *Nature* **310**, 393 (1984).
- [3] T. Loerting, C. Salzmann, I. Kohl, E. Mayer, and A. Hallbrucker, *Phys. Chem. Chem. Phys.* **3**, 5355 (2001).
- [4] P. H. Poole, F. Sciortino, U. Essmann, and H. E. Stanley, *Nature* **360**, 324 (1992).
- [5] H. Tanaka, *Nature* **380**, 328 (1996).
- [6] O. Mishima and H. E. Stanley, *Nature* **396**, 329 (1998).
- [7] O. Mishima, *Phys. Rev. Lett.* **85**, 334 (2000).
- [8] I. Brovchenko, A. Geiger, and A. Oleinikova, *J. Chem. Phys.* **118**, 9473 (2003).
- [9] E. Wilhelm, R. Battino, and R. J. Wilcox, *Chem. Rev.* **77**, 219 (1977).
- [10] L. R. Pratt, *Annu. Rev. Phys. Chem.* **53**, 409 (2003).
- [11] N. T. Southall, K. A. Dill, and A. D. J. Haymet, *J. Phys. Chem. B* **106**, 521 (2002).
- [12] D. Paschek, *J. Chem. Phys.* **120**, 10605 (2004).

- [13] K. A. T. Silverstein, A. D. J. Haymet, and K. A. Dill, *J. Am. Chem. Soc.* **122**, 8037 (2000).
- [14] R. Souda, *J. Chem. Phys.* **121**, 8676 (2004).
- [15] O. Mishima, *J. Chem. Phys.* **121**, 3161 (2004).
- [16] D. Paschek and A. Geiger, *J. Phys. Chem. B* **103**, 4139 (1999).
- [17] D. Frenkel and B. Smit, *Understanding Molecular Simulation — From Algorithms to Applications* (Academic Press, San Diego, 2002), 2nd ed.
- [18] D. Paschek and A. E. García, *Phys. Rev. Lett.* (2004), in press.
- [19] S. W. Rick, *J. Chem. Phys.* **120**, 6085 (2004).
- [20] State swapping moves between two states i and j are accepted with a probability $P_{\text{acc}} \min\{1, \exp[\beta_i(U(\vec{s}_i^N; L_i) - U(\vec{s}_j^N; L_i)) + \beta_j(U(\vec{s}_j^N; L_j) - U(\vec{s}_i^N; L_j))]\}$. Here, \vec{s}_i^N represents the set of scaled coordinates $\vec{s}_N = L^{-1} \vec{r}_N$ of the entire N -particle system belonging to state i . $U(\vec{s}_i^N; L_i)$ denotes the potential energy of configuration \vec{s}_i^N at volume $V_i = L_i^3$, whereas $U(\vec{s}_i^N; L_j)$ represents the configurational energy belonging to \vec{s}_i^N at volume V_j . The decision whether a state swapping move or an MD move is executed, is chosen at random with a probability of 0.2 to select a state swapping move.
- [21] Each replica represents a molecular dynamics (MD) simulation of 256 molecules in the *NVT* ensemble. The electrostatic interactions are treated by the Ewald summation [34] with a real space cutoff of 0.9 nm and a $18 \times 18 \times 18$ mesh with 4th order interpolation for the reciprocal lattice contribution. Lennard-Jones cutoff corrections for energy and pressure have been taken into account. A 2 fs timestep was used. The simulations were carried out using the GROMACS 3.2 code [35], modified by us in order to allow for V, T -state-swapping moves. The temperature tiling has been chosen to maintain an acceptance ratio of about 0.2 for state swapping.
- [22] W. Wagner and A. Prüß, *J. Phys. Chem. Ref. Data* **31**, 387 (2002).
- [23] M. Yamada, S. Mossa, H. E. Stanley, and F. Sciortino, *Phys. Rev. Lett.* **88**, 195701 (2002).
- [24] P. H. Poole, private communication.
- [25] M. C. Bellissent-Funel, J. Teixeira, and L. Bosio, *J. Chem. Phys.* **87**, 2231 (1987).
- [26] J. L. Finney, A. Hallbrucker, I. Kohl, A. K. Soper, and D. T. Bowron, *Phys. Rev. Lett.* **88**, 225503 (2002).
- [27] R. P. Kennan and G. L. Pollack, *J. Chem. Phys.* **93**, 2724 (1990).
- [28] R. Fernandez-Prini and R. Crovetto, *J. Phys. Chem. Ref. Data* **18**, 1231 (1989).
- [29] S. Garde, G. Hummer, A. E. García, M. E. Paulaitis, and L. R. Pratt, *Phys. Rev. Lett.* **77**, 4966 (1996).
- [30] D. Paschek, *J. Chem. Phys.* **120**, 6674 (2004).
- [31] When fitting the original data for Ar of Ref. [27].
- [32] G. Hummer, S. Garde, A. E. García, and L. R. Pratt, *Chem. Phys.* **258**, 349 (2000).
- [33] D. Huang and D. Chandler, *Proc. Natl. Acad. Sci. USA* **97**, 8324 (2000).
- [34] U. Essmann, L. Perera, M. L. Berkowitz, T. A. Darden, H. Lee, and L. G. Pedersen, *J. Chem. Phys.* **103**, 8577 (1995).
- [35] E. Lindahl, B. Hess, and D. van der Spoel, *J. Mol. Model.* **7**, 306 (2001).